ANVESAK
ISSN: 0378–4568 UGC Care Group1 Journal

ANALYSIS ON FINITE ELEMENT METHOD APPLIED TO DETERMINE THE FAULT CURRENT OF CONNECTED AND NON-CONNECTED BROKEN ROTOR BARS OF INDUCTION MACHINE

[1] T. Sreekanth, [2] V. Vishnu Vardhan, [3] O.Thireesh, [4] K Girish Kumar
[1,2,3,4] Dept of Electrical and Electronics Engineering, Sree Venkateswara College Of Engineering, Nellore (Dt), Andhra Pradesh, India.

ABSTRACT
Induction motors are extensively worn in production manufacturing which is drive for different industrial loads. The failure of these motors results in expensive maintenance and revenue losses. In three-phase squirrel-cage induction motors, broken rotor bars and end-rings faults can damage the machine and to be replaced which increases the capital cost. BRB are due to frequent on and off of the motor, manufacture defect, and transient loading conditions. These defects produce un even flux distribution, distorted current spectrum, and torque oscillations. The finite element method (FEM) is a numerical study to determine the presentation of the machine with BRB currents. The software ALTAIR FLUX is used to model a mutually healthy and broken rotor cage here. With the aid of simulation findings, the magnetic flux distribution and magnetic flux density are seen as well as the current response of healthy and broken rotor bars. Finally, inter bar currents caused by broken rotor bars enhance the strength of the currents in healthy bars next to and far from them, which can lower the machine's performance and life span.

1. INTRODUCTION

Heavy-loaded induction motors are more prone to flaws like broken rotor bars and end rings, which cause the squirrel-cage rotor to be asymmetrical, especially those that, are often started and stopped. Such flaws disrupt the working of the motor and reduce its life span. As a result, diagnosing and detecting defects in induction motors can help to maintain the motor's high performance and normal lifetime. Diagnosing and detecting defects in induction motors can help to maintain the motor's high performance and normal lifetime. Induction machine failures are typically classified into three primary classes base on the major machine apparatus namely, bearing, stator, and rotor defects. A number of independent investigations have found, bearing failures account for around of all defects related with induction devices. Meanwhile, stator winding defects account for an additional of induction machine failures. Although the processes of stator and bearing failuresvariessomewhatacrossdissimilarcategoryofelectricmachines,here defects are recognized by prevalent trouble in different forms of electric machines, such as synchronous, brush less dc, hesitancy, and so o in addition,rotorfailuresversionroughlyofallinductionmachineoccurrence.Thesedefects,however,areuniquetosquirrelcage induction motors, as contrasted to bearing and Stator faults.

Inter-laminar currents, also known as inter bar currents, induced as default sin the rotor core plates.

1) Rotor end-ring coupling failures. 2) Rotor bar failures.

These defects can be caused by arrange of stressors as well as manufacturing flaws. Frequent thermal and electrical.

Major Faults in IM	IEE-IAS (%)	ERPI (%)	ALLIANZ (%)
Bearing	44	41	13
Stator Windings	26	36	66
Rotor Bars	8	9	13
Miscellaneous	22	14	8

Table1: Main faults associated to dissimilar surveys

Over loading, plus extreme vibrations caused by provide voltage unbalances, load variations, and predominant protrusive transients, can causes quirrel-cage rotor bars and added structural apparatus to fail more quickly.

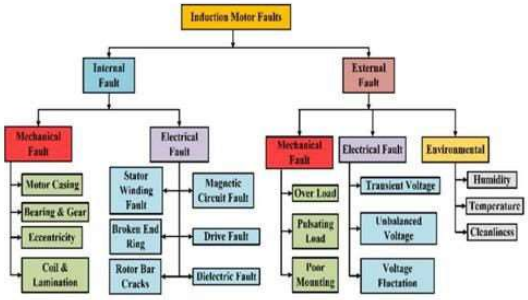

Fig1: Different faults in IM

Here, only the issue of the shattered squirrel cage bars is addressed. Further investigation is done into the effects of neighboring and non-adjacent faults on two previously proposed rotor fault diagnosis techniques..

2. ROTOR BROKEN BARS

In three-phase squirrel-cage induction motors, cracked or fractured rotor bars and end-rings are common problems.Rotorbarsfaultsareaddedcommonthanmoldedrotorfaults.Itissimpletorepairtheformerrotorbar.Thete mperaturerise around the damaged bars can finally break the bars, resulting in an electric arc in the area. The plates on the rotorbody around the broken bars may suffer damage as a result. Because of this, the current from the wrecked bar is transmitted to nearby bars, increasing the tension and current flow. As a result, when a rotor bar breaks in this location, the other bars are compelled to contest the flaw caused by the intense applied pressure. It implies that future bars may break after a little period of time following the first broken bar.

Fig 2: Healthy rotor bar

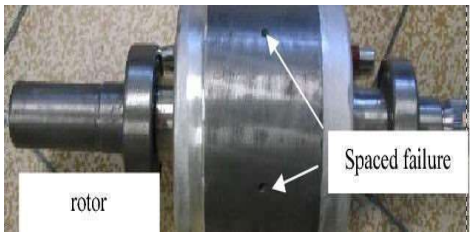

Fig 3:Two Adjacent Broken Rotor Bars of IM Fig 4: Two Non-Adjacent Broken Rotor Bars of IM The next explanation is for cracked or fractured rotor bars: excess, uneven heat distribution, hotspots, and arc calls causing mechanical stress. Magnetic strains are brought on by electromagnetic vibrations, electromagnetic forces, and magnetic asymmetry forces. Residual stress connected to the fabrication process. Dynamics stress is brought on by centrifugal and rotor axial torque. Humidity, rotor wear, chemical contamination, and circumferential tension Mechanical stress brought on, among other things, by the loosening of laminates, ball bearing damage, and mechanical depletion of various parts.

A healthy motor with two dispersed models and a cage rotor is shown in Fig. 5. The loop is created by two neighboring bars, as shown. The dispersed model of a rotor cage is seen as a rotor bar is wrecked. The currents of the two loops that make up the projected bar are comparable, as shown in Fig. 6.

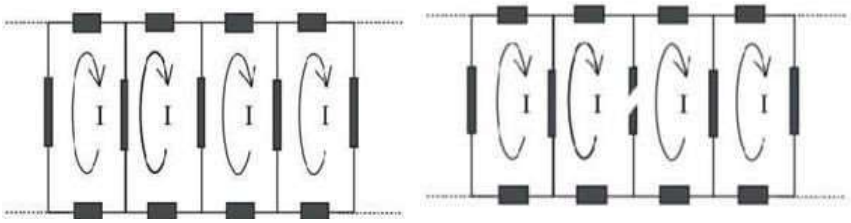

Fig 5: Distributed Rotor Cage in Induction Motor Fig 6: Distributed Rotor Cage in Rotor Cage by One BRB

3. METHODOLOGY Finite Element Method

The ideal strategy for designing any kind of electrical equipment is to use the finite element method (FEM), which is a recognized approach for numerically solving differential equations in engineering and mathematical modelling.

Back ground of FE method

The FE approach has its origins in structural analysis. In 1968, the FE approach was first used to electromagnetic difficulties [8]. Maxwell's equations govern the pattern of electromagnetic fields in electromagnetic devices. Understanding the behavior of electromagnetic devices requires solving Maxwell's equation, which is a difficult task. This problem was addressed by combining a numerical approach (the FE method) with computer-assisted computing. In basic words, it is the process of employing computers to solve differential equations using numerical techniques. The domain is the name given to the region of interest in the FE approach. The field is separated keen on lesser sub domains or elements, each of which has its own set of equations to solve, yielding a solution [8]. The FEA is a key technique for understanding the electromagnetic behavior of spinning electric gear. Many creative concepts are validated via FE modelling. A multitude of software packages are presently used to perform FEA on electrical gear. **Summary of solve the FE problem**

Present segment gives an summary of the FE issue formulation and solution process. The first step in every FE issue is to write out the equations that describe the system's general physics. The electromagnetic fields that regulate the functioning of electrical devices are of primary importance. Since the laws of electricity and magnetism are included, the Maxwell equations (2.1) - (2.4), which are 4 linked partial differential equations, serve as the foundation. In the equations (2.1 to 2.4), D stands for movement electric field, B for magnetic flux density vector field, E for electric field intensity vector field, H for magnetic field intensity vector field, and J for current density vector field.

The electromagnetic field behavior for places where the current density is determined may be examine during (2.6).However, in the case of an induction machine, the current is provoked in the rotor bars, therefore the information regarding J is unknown beforehand. This issue is overcome with (2.3). By switching (2.5) for (2.3) and further simplifying, we arrive at:

$E = -\partial A\ \partial t - \nabla Vpot$

(2.7) where Vpot is the electric scalar potential by means of the relationship J= σE

We get at the absolute formulation, that would be used in the numerical synthesis of electric machine, by adding (2.6) to (2.7), where is the electrical conductivity. In the sentence (2.8),

∇V pot signify the applied voltage to the system.

$$\nabla 2A\ \mu - \sigma\ \partial A\ \partial t = -J + \sigma \nabla Vpot \qquad (2.8)$$

FE modeling of rotor

The rotor circuit must then be represented in FE software using the provided summary. The inductance machine's rotor is made up of rotor bars, rotor core, shaft, and rotor slot wedge. As the first step in rotor modelling, the shape of various portions and the accompanying material properties are produced. A new method for estimating the size of the rotorbars had to be developed as the geometrical data for the rotorbars was missing.

4. RESULTS

The subsequently step is to utilize the provided brief description to model the rotor circuit in FE software. The rotor of an induction machine is made up of rotor bars, rotor core, shaft, and rotor slot wedge. The geometry of various parts, as well as their associated material properties, is produced as the first step of rotor modeling. Due to the lack of geometrical data for the rotor bars, an method for estimating rotor bar size has to be established.

Type of Machine	2-pole Induction Motor
Type of Connection	3-Phase Star
Rated Load Power	7.5KW
Rated Source Voltage	380V
Rated Source Frequency	50Hz
Stator Armature Slots	20
Rotor Armature Slots	24

Table 2: Specifications of IM

Using Altair Flux Software the above stator winding was designed by considering 24 slots instator.

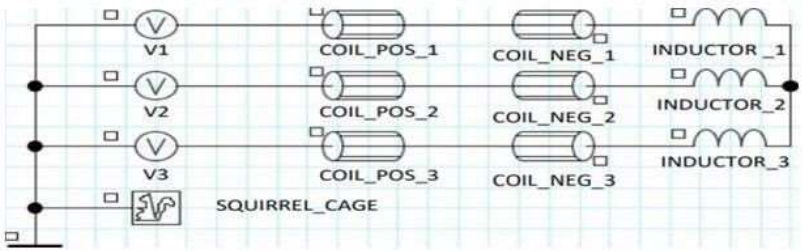

Fig:7 Electrical path of the inductance motor

The above Fig-7is the electrical path of the Inductance motor which is three-phase and the rotor type is squirrelcage.

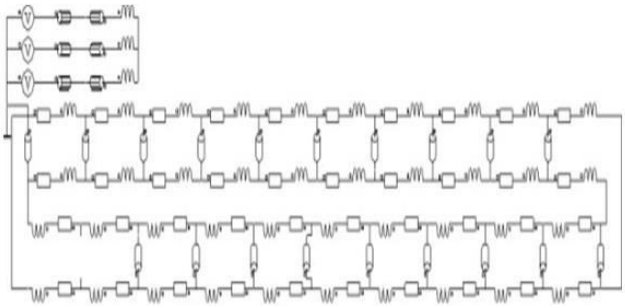

Fig-8 The electrical circuit associated to the finite element model for broken bar

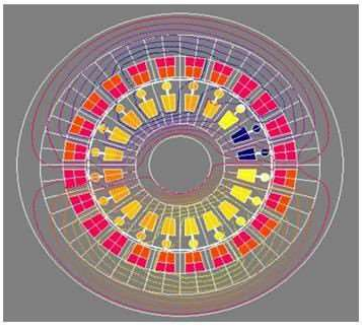

Fig9: Meshing of Induction Motor

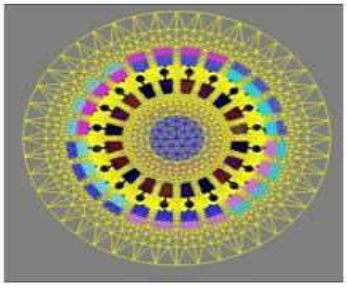

Fig10: Meshing of Induction Motor

The Uneven Flux Distribution caused by Two Adjacent Broken Rotor Bars of an Inductance Motor is seen in the diagram above. The neighboring broken rotor bars, barno. 19 and barno. 20, are marked with the blue hue in the above fig.

Fig11: current response in rotor barno:19

The above fig: 11 represents the current response in rotor barno:19 which is assumed as broken in the Induction motor.

The X-axis symbolizes the Resistance and the Y-axis symbolizes the current.

Fig:12 current response in rotor barno:20

The above fig: 12 represent the current response in rotor barno: 20 which is assumed as broken in the Induction motor. The X-axis symbolize the Resistance and the Y-axis symbolize the current

Fig:13 Current response in rotor barno:1

The above fig:13 represent the current response in rotor barno:1 because of the effect of neighboring broken rotor bars of an Induction motor. The X-axis symbolizes the Resistance and the Y-axis symbolizes the current.

Fig:14 Current response in rotor barno:18

The above fig 14 represents the current response in rotor bar no: 18 due to the effect of adjacent broken rotor bars of an Induction motor. The X-axis symbolizes the Resistance and the Y-axis symbolizes the current.

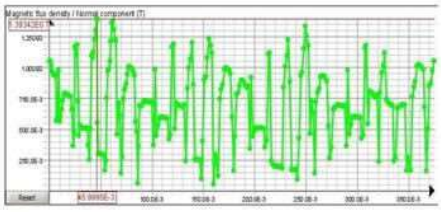

Fig. 15: Graphical illustration of the flux pattern in IM as a result of nearby fractured rotor bars The above fig:15 represent the Graphical representation of Flux distribution in IM due to the effect of adjacent broken rotor bars. the resistance along the X-axis and the current along the Y-axis.

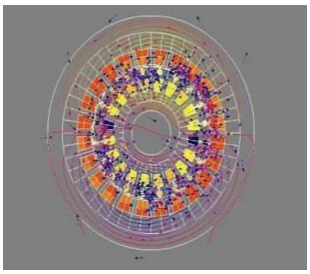

Fig:16 Un-even flux distribution due to2 Non-adjacent broken rotor bars

The above fig: 16 represent the Uneven Flux distribution due to 2 Non-Adjacent Broken Rotor bars of an Induction motor. The bar no: 10 and bar no: 20 are the non-Adjacent broken rotor bars as indicated by blue color as represented in the above fig: 15.

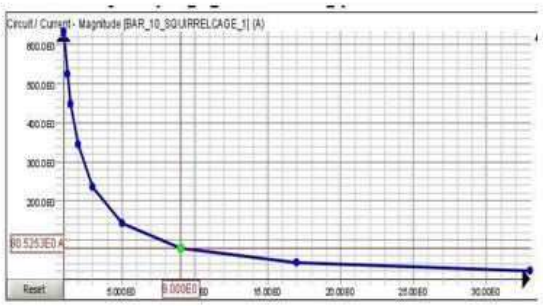

Fig17: Current response in rotor barno:10

The above fig: 17 represent the current response in rotor barno: 10 due to the effect of non-Adjacent broken rotor bar so fan Inductance motor. The X-axis symbolizes the Resistance and the Y-axis symbolizes the current.

Fig18: Current response in rotor bar no:20

The above fig: 18 symbolizes the current response in rotor bar no: 20 due to the effect of non-Adjacent broken rotorbarsofanInductancemotor.TheX-axissymbolizestheResistanceand the Y-axis symbolizes the current.

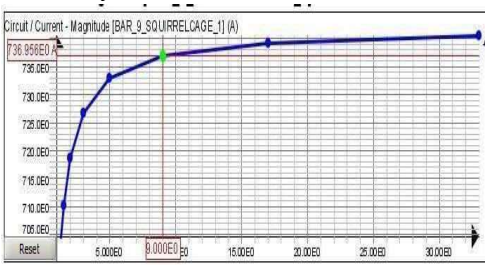

Fig19: Current response in rotor bar no:9

The above fig: 19 represents the current response in rotor bar no: 9 because of the result of broken rotor bar number 10 of an Induction motor. The X-axis symbolizes the Resistance and the Y-axis symbolizes the current.

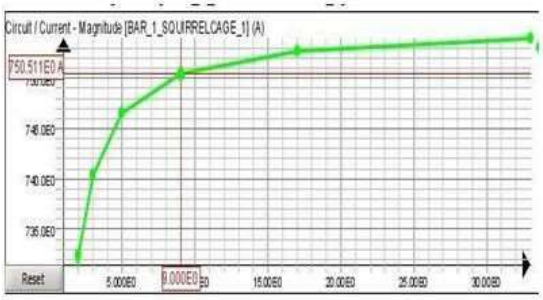

Fig20: Current response in rotor bar no:11

The above fig: 20 represents the current response in rotor bar no: 11 owing to the result of broken rotor bar number 10 of an Induction motor. The X-axis symbolizes the Resistance and the Y-axis symbolizes the current.

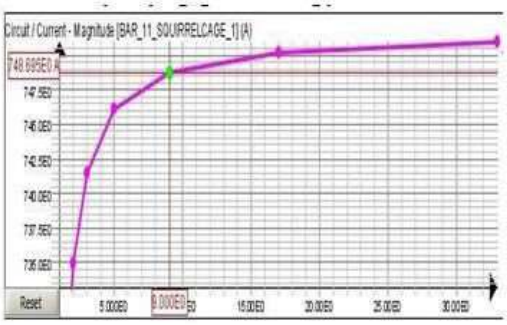

Fig21:Current response in rotor bar no:1

The above fig: 21 represents the current response in rotor bar no: 1 because of the result of broken rotor bar number 20 of an Induction motor. The X-axis symbolizes the Resistance and the Y-axis symbolizes the current.

Fig22: Current response in rotorbarno:19

The above fig: 22 represents the current response in rotor bar no: 19 since of the result of broken rotor bar number 20 of an Induction motor. The X-axis symbolizes the Resistance and the Y-axis symbolizes the current.

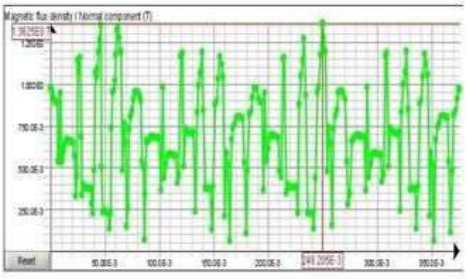

Fig: 23 Graphical representation of Flux distribution in IM due to the result of Non-adjacent broken rotor bars

Fig 23: represents the Graphical representation of Flux distribution in IM due to the effect of non-adjacent broken rotor bars. The X-axis symbolizes the Resistance and the Y-axis symbolizes the current.

CONCLUSION

In this Paper, A squirrel cage induction motor with healthy, adjacent, and non-adjacent fractured rotor bars is simulated using the Finite Element Method (FEM). This research projects a fresh movement for the perception of damaged rotor bars depending on the presence of inter bar currents. The project makes the assumption—and finally proves it—that inter bar currents work in concert with stator flux density to drive the rotor axially. In squirrel-cage inductance machines, the effects of nearby and non-adjacent bar breakages on rotor faulting detection were looked at. However, some designs of squirrel cages is more susceptible to these nonadjacent happening. Low-rotor-bar squirrel cage rotor systems, like the one that was the subject of this study, may be at danger of failure.

Currentinrotorbar:19	101.21A
Current in rotor bar :20	94.37A
Current in rotor bar :18	834.71A
Current in rotor bar :1	814.18A

Table 3: Comparison for the current responses due to adjacent BRB.

Currentinrotorbar:10	80.52A
Currentinrotorbar:20	82.48A
Currentinrotorbar:9	736.95A
Currentinrotorbar:11	748.69A
Currentinrotorbar:19	740.43A
Currentinrotorbar:1	750.51A

Table 4: Comparison for the current responses due to non-adjacent BRB.

REFERENCES

1. A.H. Bonnett and G. C. Soukup, Analysis of rotor failures in squirrel-cage induction motors, IEEE Trans. Ind.Appl., vol. 24, no. 6,pp.1124–1130,Nov./Dec.1988.
2. R. F. Walliser and C. F. Landy, Determination of interbar current effectsin the detection of broken rotor bars insquirrelcage inductionmotors,IEEETrans. EnergyConversion,1994.
3. Prasad,KapuV.SriRam,andVarshaSingh,FiniteElementAnalysisforFaultDiagnosisinBrokenRotorBarof aPolyphaseInductionMotor,*SecondInternationalConferenceonPower,ControlandComputingTechnologies(ICPC2T)*.IEEE,2022.
4. Diagnosis and characterization of effects of broken bars and connectors in squirrel-cage induction motors by atime-steppingcoupledfiniteelementstatespacemodelingapproach,IEEETrans.EnergyConversion,1999.
5. A.H.BonnettandT.Albers,Squirrel-cagerotoroptionsforACinductionmotors,IEEETrans2001.

6. Diagnosis and characterization of effects of broken bars and connectors in squirrel-cage induction motors by atime-steppingcoupledfiniteelementstatespacemodelingapproach,IEEETrans.EnergyConversion,1999.
7. Prasad, Kapu V., and Varsha Singh, Numerical investigation and experimental modal analysis validation tomitigate vibration of induction machine caused due to electrical and mechanical faults. Journal of ElectricalEngineering &Technology,2022.
8. J.F.BanguraandN.A.Demerdash,Comparisonbetweencharacterizationanddiagnosisofbrokenbars/endringconnectorsandairgapeccentricitiesofinductionmotorsinASD'susingacoupledfiniteelementspacemethod,IEEETrans. EnergyConversion, 2000.
9. Prasad,KapuV.SriRamPrasad,andVarshaSingh.LoosenessIdentificationofStatorEndWindingsofInductionMotor by Modal Test. 2020 IEEE International Conference on Power Electronics, Drives and Energy Systems(PEDES). IEEE, 2020.
10. Yazici and G. B. Kliman, an adaptive statistical time-frequency method for detection of broken bars and bearingfaultsinmotorsusingstator current, IEEETrans. Ind. Applicat, 1999.
11. S. T. J. Manolas and J. A. Tegopoulos, Analysis of squirrel cage induction motors with broken bars and rings,IEEETrans. EnergyConversion, 1999.
12. Milimonfared, H. M. Kelk, S. Nandi, A. D. Minassians, and H. Toliyat, A novel approach for brokenrotor-bardetectionincage inductionmotors,IEEETrans. Ind. Applicat,1999.
13. N. M. Elkasabgy, A. R. Eastham, and G. E. Dawson, Detection of broken bars in the cage rotor on an inductionmachine, IEEE Trans. Ind. Applicat,1992.
14. Prasad,KapuV.SriRam,andVarshaSingh.LoosenessIdentificationofStatorEndWindingsofInductionMotorby ModalTest. 2020 IEEE International Conference onPowerElectronics, Drives andEnergy Systems(PEDES). IEEE, 2020.
15. G. B. Kliman, R. A. Koegl, J. Stein, R. D. Endicott, and M. W. Madden, Noninvasive detection of broken rotorbarsinoperatinginductionmotors,IEEETrans. EnergyConversion,1988.